Supporting materials to

«Ultra-bright and narrow-band emission from Ag atomic sized nanoclusters in a self-assembled plasmonic resonator»

Anton S. Gritchenko,[1] Alexey S. Kalmykov,[1] Boris A. Kulnitskiy,[2,3] Yuri G. Vainer,[1] Shao-Peng Wang,[4] Bin Kang,[4] Pavel N. Melentiev,[1,*] Victor I. Balykin[1]

[1]Institute of Spectroscopy RAS, Moscow, Troitsk 108840, Russia

[2]Technological Institute for Superhard and Novel Carbon Materials, Moscow, Troitsk 108840, Russia

[3]Moscow Institute of Physics and Technology, Moscow reg., Dolgoprudny, 141700, Russia

[4]State Key Laboratory of Analytical Chemistry for Life Science and Collaborative Innovation Center of Chemistry for Life Sciences, School of Chemistry and Chemical Engineering, Nanjing University, 163 Xianlin Road, Nanjing 210023, P. R. China

*Corresponding author's e-mail: melentiev@isan.troitsk.ru

Section 1. Electron diffractometry of samples

Figure S1 shows the electron diffraction pattern obtained by transmission electron microscope (TEM) JEOL JEM 2010 (Technological Institute of Superhard and Novel Carbon Materials, Moscow, Troitsk). The accelerating voltage was set to 200 kV, the sample area was 100 nm × 100 nm.

Each single bright point corresponds to the maximum of electron beam diffraction on different Ag nanoparticles and Ag nanoclusters of the sample. The absence of crystallographic directions indicates a polycrystalline structure of the sample [1]. The diameters of the rings correspond to the crystal lattice of silver.

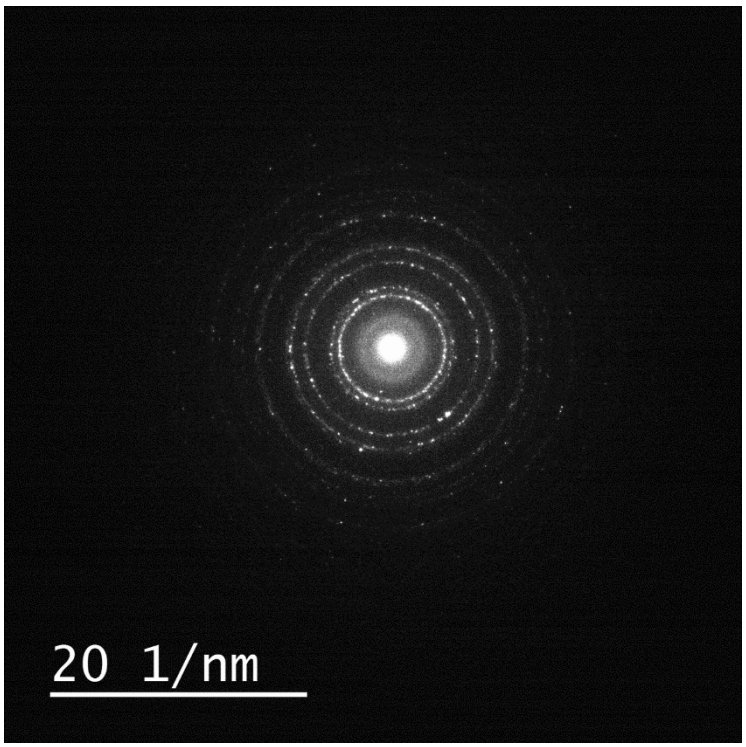

Figure S1. Electron diffraction pattern of sample containing Ag nanoclusters in GPC.

Section 2. TEM microscopy of samples

TEM images were acquired using a transmission electron microscope JEOL JEM 2010 (Technological Institute of Superhard and Novel Carbon Materials, Moscow, Troitsk). The accelerating voltage was set to 200 kV.

Samples for TEM microscopy and electron diffraction were obtained by thermal vapor deposition of silver atoms on 40 nm thin quartz membranes (Ted Pella). The thickness of the silver film is estimated to be 15 nm, and the average size of the nanoparticles varies between 50 and 200 nm.

In the high-resolution regime, one can clearly see the formation of small (less than 10 nm) silver nanoclusters. On larger nanoclusters, with size larger than 3 nm, the diffraction pattern of the silver lattice can be seen (Figure S2a,b). However, smaller particles do not show this feature, due to the limitations of JEM 2010 TEM. In some regions, single nanoclusters can be found between silver nanoparticles (Figure S2a), at the same time groups of nanoclusters can be observed in other gap plasmon cavities (Figure S2b).

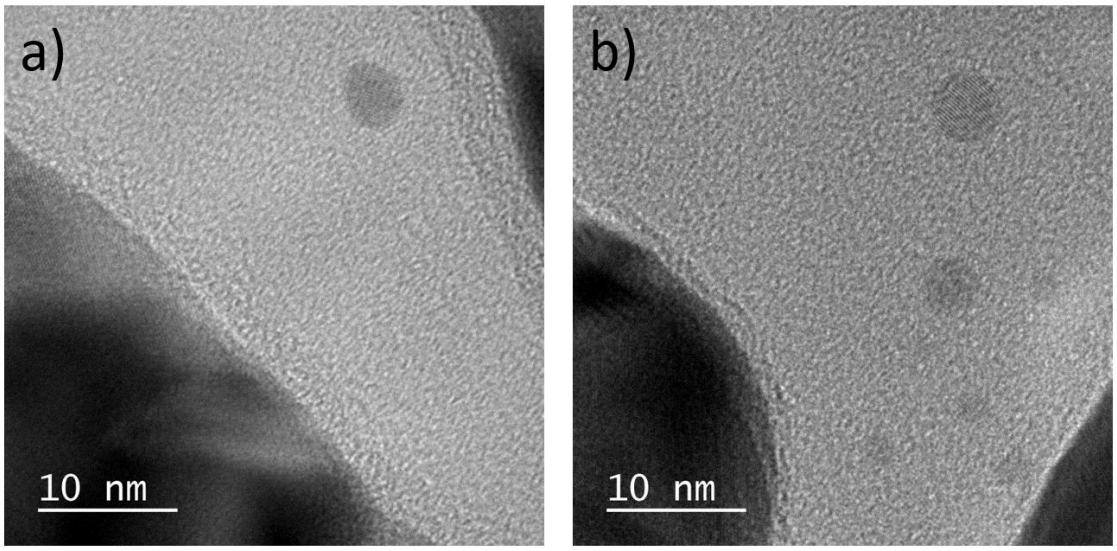

Figure S2. TEM microscopy of Ag nanoclusters located between Ag nanoparticles.

Section 3. Transmission of gap-plasmon cavity

Figure S3 shows transmission spectrum recorded using a xenon arc lamp for white light illumination. The spectrum consists of a broad band typical of plasmonic resonances of gap structures [2] and narrow dips at 540 nm and 575 nm, which may correspond to resonances of silver nanoclusters.

White light was focused on the sample with the 10x Nikon Plan Fluor objective, and the transmitted light was collected with the Nikon 100x objective and imaged onto the entrance of the optical fiber with 100 μm core diameter. The transmission spectrum was recorded using a grating spectrometer coupled to Hamamatsu C-9100 EMCCD camera.

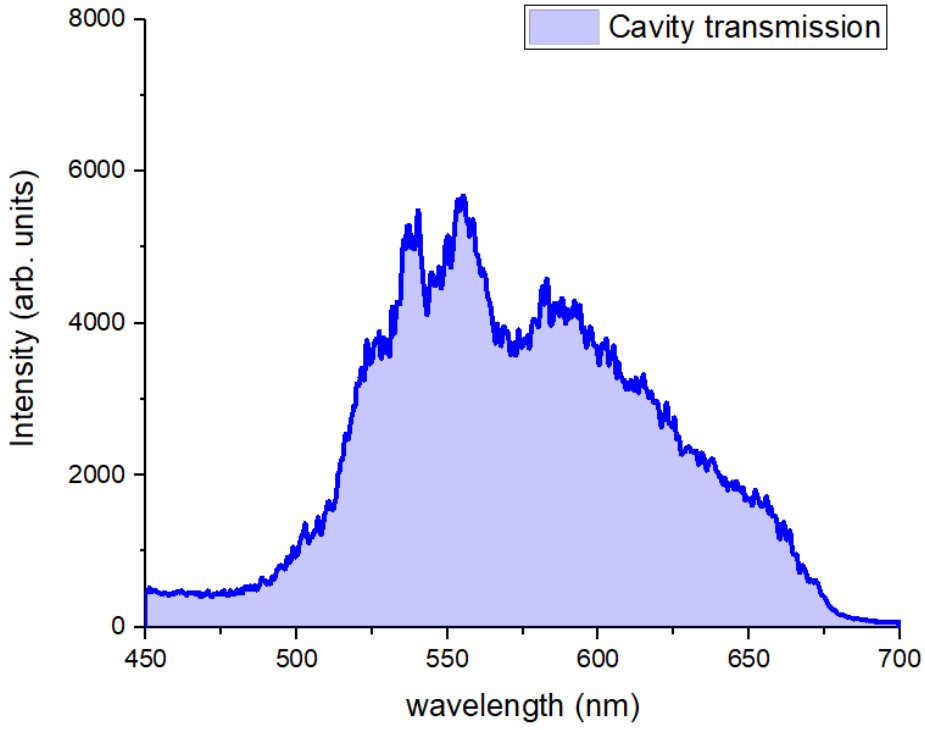

Figure S3. Transmission spectra of gap-plasmon cavity (GPC) resonator

Section 4. Temporal kinetics of emission spectra

The blinking of nanoclusters in the GPC is accompanied by a change in the emission spectrum (see Figure S4). The entire emission spectrum consists of many narrower lines that turn on and off with time. This can be explained by the fact that many nanoclusters of different sizes are present in the GPCs at the focused spot of the laser. Each nanocluster has its own but usually similar energy structure. However, one of the lines dominates in the spectrum. This line may be the same for nanoclusters of different sizes, but this explanation requires further investigation.

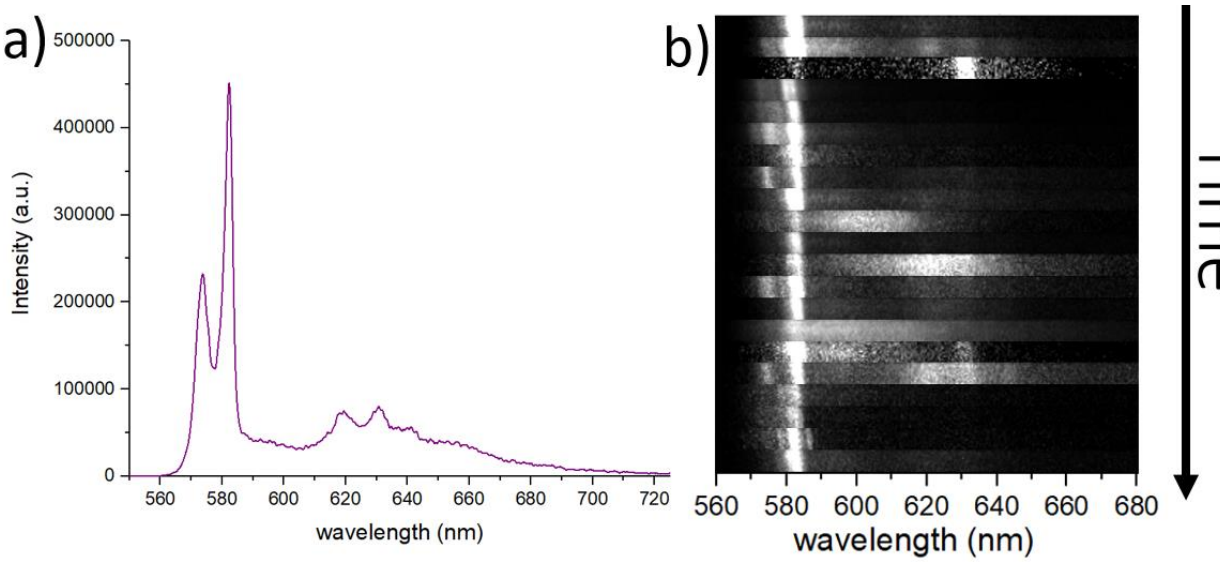

Figure S4. Temporal dynamics of the Ag nanocluster in GPC resonator spectrum: (a) overall spectrum obtained by rolling averaging of 256 frames with 100 ms exposure for each frame, (b) individual frames.

Section 5. Experimental setup

The experimental setup (Figure S5) is based on a Nikon Ti/S inverted optical microscope. Different lasers were used to excite the fluorescence of the Ag nanoclusters: (1) 520 nm (Thorlabs, PL520), (2) 532 nm (Lighthouse Photonics Sprout G) and (3) 520 -540 nm, 1.5 ps tunable Ti:Sa picosecond laser system Coherent Mira - OPO for wavelength dependent measurements. The laser beam from the pulsed laser was transmitted through a 50 μm single-mode fiber, and the pulse duration after the fiber was 6 ps. To filter the laser light, a dielectric short-pass filter was inserted into the filter cube. The laser light was focused to a diffraction-limited spot using a Nikon dry objective (x100, NA 0.95). The sample containing the Ag nanoclusters was arranged in a 2D piezo translation stage with an accuracy of 10 nm (PiezoJena). The radiation of the Ag nanoclusters in the GPC resonator was recorded with the same objective. The radiation from the Ag nanoclusters was filtered from the laser light using a dichroic mirror (DMLP 567, Thorlabs), a long-pass filter (FELH 550, FEL550, Thorlabs), and a color filter (OS -13). The filtered light was focused on the Hamamatsu ORCA CMOS camera or passed through the aperture in the Hanbury-Brown and Twiss confocal scheme. Transmission measurements were made using xenon arc lamp.

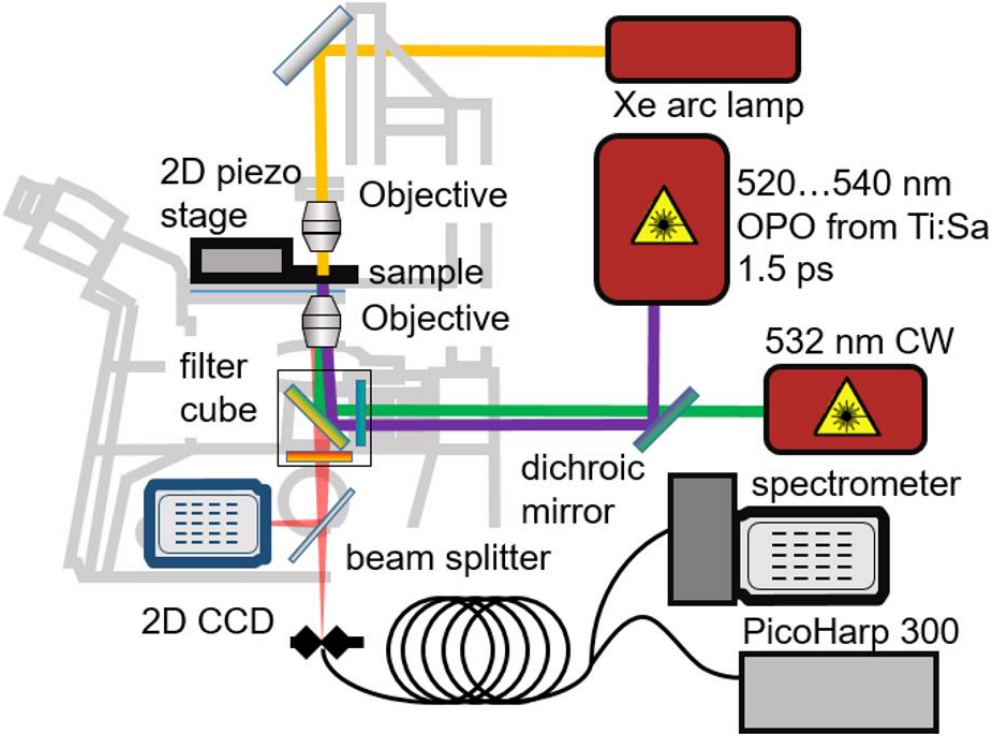

Figure S5. Experimental setup scheme.

Fluorescence lifetime and temporal autocorrelation measurements were performed using the Hanbury-Brown and Twiss system equipped with MPD Avalanche photodiodes and the PicoHarp 300 TCSPC system. The synchronous signal for the lifetime measurements was obtained using the APD210 Avalanche photodiode from Menlo Systems. The autocorrelation function was measured in the T2 regime[2].

Spectral measurements were performed using commercial grating spectrometer with a spectral resolution of 1 nm and a homemade spectrometer with a resolution of 0.06 nm. Both spectrometers were equipped with a Hamamatsu c-9100 EMCCDs.

Section 6. Measurements at different wavelengths of the exciting laser light

Both the spectral (Figure S6a) and power (Figure S6b) dependence of the fluorescence spectrum of Ag nanoclusters show linear behavior. From these results, the Raman nature of the radiation can be inferred. However, the intensities of Ag clusters in GPC fluorescence are several orders of magnitude higher than those of surface-enhanced Raman scattering [3, 4]. Moreover, one of the necessary conditions for the Raman mechanism is the presence of vibrational energy levels [5], which is not the case for Ag nanoclusters in the GPC system.

Another feature of the radiation from nanoclusters in GPC is the multiline structure of the fluorescence spectrum. It consists of many lines with FWHM of 1 nm or less. This can be explained by the presence of many Ag nanoclusters of different sizes in a diffraction-limited laser spot. Each of the clusters has its own energy structure, which is slightly different from that of other nanoclusters. Each of them produces its own line in the overall spectrum, which can also be explained by measurements of the temporal dynamics of the spectrum (Figure S4).

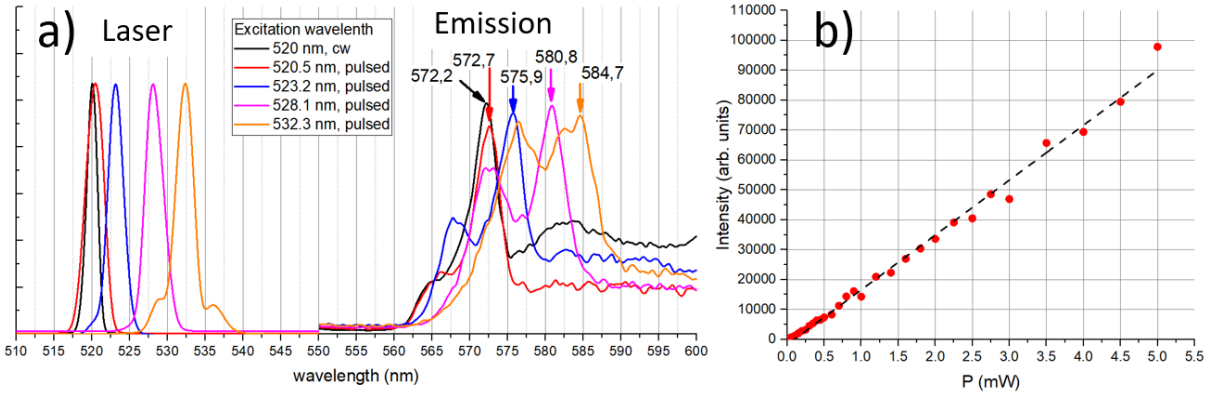

Figure S6. Measurements at different wavelengths of the exciting laser light: (a) dependence of the fluorescence spectrum of Ag nanoclusters on the excitation wavelength; (b) dependence of the intensity of the narrow lines on the power of the excitation laser.

Section 7. Polarization properties of the Ag clusters emission

Another feature of Ag nanoclusters found in the fluorescence of GPC resonators is the strong polarization of the emission. The intensity of the fluorescence of the narrow lines forming the total spectrum depends on the angle between the polarizer and the analyzer used in the experimental setup. This may be caused by the anisotropy of the GPC, which has a strong field enhancement perpendicular to the slit and a low enhancement in the parallel direction. We see that the maximum intensity of the 581-nm line is obtained when the polarization is almost perpendicular to that of the 575-nm line (Figure S7a), which can be explained by the dependence of the GPC resonance on an arbitrary angle with respect to the polarization of the excitation laser light [6]. When the GPC resonance is shifted to the blue region of the spectrum, the blue line (575 nm) of Ag nanoclusters exhibits a higher gain factor (Figure S7b). When the resonance shifts to the red line (581 nm), it starts to dominate in the spectrum.

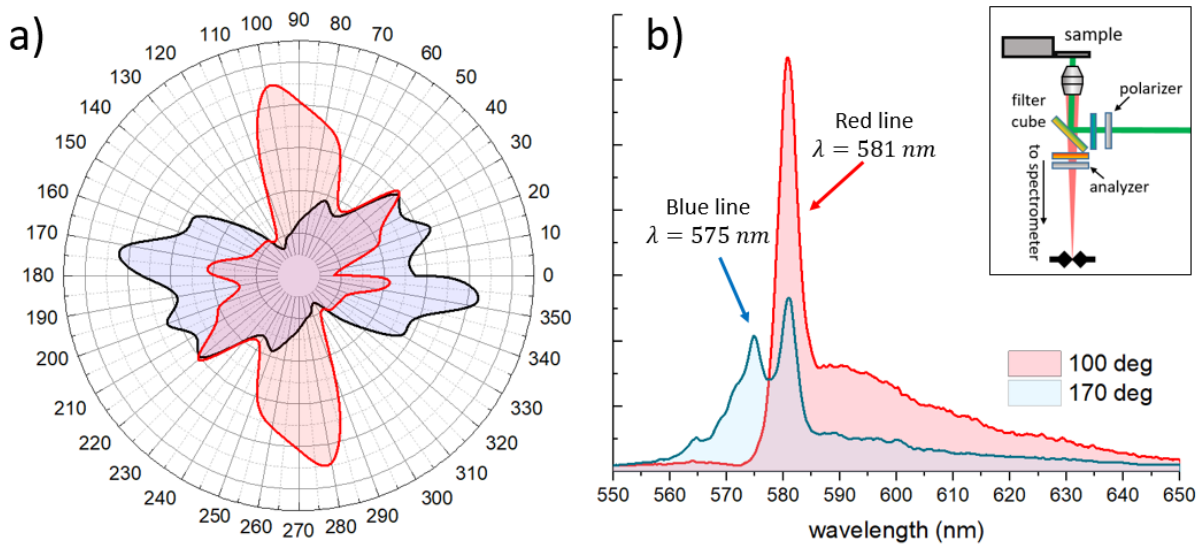

Figure S7. Polarization properties of Ag cluster emission in GPC resonator: (a) analysis of two Ag nanoclusters emission lines (575 nm and 581 nm) with polarization analyzer; (b) overall spectrum of Ag nanoclusters fluorescence measured with different angles between polarizer and analyzer.

Section 8. Fluorescence cross-section of Ag nanoclusters

We define the fluorescence cross-section as $\sigma_{em} = \sigma_{abs} \times \eta$, where η is fluorescence quantum yield. It can be measured experimentally as $\sigma_{em} = P_{em}/I_{inc}$, where $I_{inc} = 30\ kW/cm^2$- excitation intensity, P_{em} – nanocluster emission power. Nanocluster emission power was measured using SPAD, as photon flux and recalculated in the units of power [W]: $P_{em} = \Phi_{SPAD} \times \hbar\omega\ /\eta_{SPAD} \times \eta_{microscope}$, where Φ_{SPAD} – photon flux registered by SPAD, η_{SPAD} – SPAD quantum efficiency, $\eta_{microscope}$ – microscope collection efficiency including losses on its elements, $\hbar\omega$ – energy of single photon with the wavelength $\lambda = 580\ nm$.

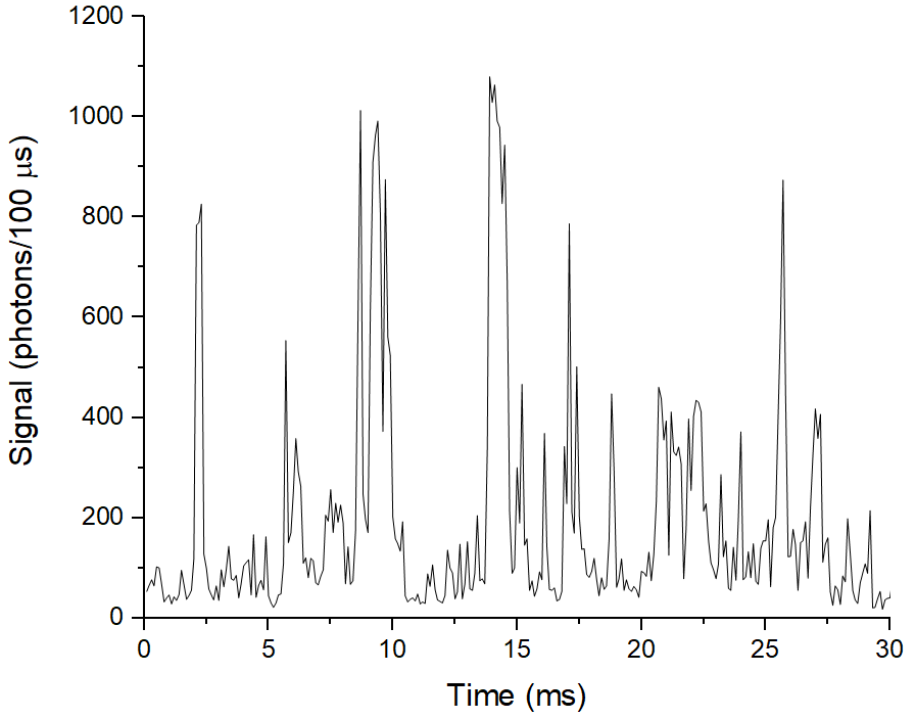

Figure S8. Timetrace of nanoclusters fluorescence with $I_{inc} = 30\ kW/cm^2$.Photon flux peaks at $\Phi_{SPAD} = 10^7\ \frac{phot}{s}$.

Thus, $\sigma_{em} = \frac{P_{em}}{I_{inc}} = \frac{10^7 \frac{phot}{s} \times 2.13 \times 1.6 \times 10^{-19} J/phot}{0.5 \times 0.035 \times 3 \times 10^4\ W/cm^2} \approx 0.7 \times 10^{-14}\ cm^2$, where $2.13 \times 1.6 \times 10^{-19} J/phot$ – single photon energy in Joules, SPAD photon flux $\Phi_{SPAD} = 10^7 \frac{phot}{s}$ (рис.).

This parameter was confirmed by comparing the emission of silver nanoclusters and a single NV center in nanodiamond. For a single NV center, the photon flux under the same excitation conditions ($I_{inc} = 30\ kW/cm^2$) using the same detection scheme was $\Phi_{SPAD} = 5 \times 10^3 \frac{phot}{s}$. It is known from the literature that the fluorescence cross section of NV center $\sigma_{em} = 4.9 \times 10^{-17} cm^2$ [7] and the quantum yield for NV centers in nanodiamonds is of the order $QY \sim 0.1$ [8]. This means that the fluorescence cross section of nanoclusters is 200 times larger than the fluorescence cross section of NV centers in nanodiamond and can be estimated as $\sigma_{em} \approx 10^{-14}\ cm^2$.

The emission cross section can be calculated using the Fuechtbauer-Ladenburg equation adapted for the Gaussian form of spectral density [9]. The equation can be written as $\sigma_{em}(\lambda) = \sqrt{ln2/\pi} \frac{\lambda^2}{4\pi n^2} \frac{\eta}{\tau_{GPC}} \frac{1}{\Delta\nu}$, where λ – peak wavelength of the emitter, τ_{GPC} – emission lifetime, $\Delta\nu$ – FWHM of the spectrum in Hz, η – quantum yield, n – refractive index of the medium. However, a direct comparison of the calculated cross section with the measured value is not straightforward for several reasons: (1) the value of the refractive index n remains unclear for such complex systems as a nanocluster located in the gap plasmon cavity; (2) the complex spectral kinetics, the emission of spectral lines at different wavelengths at different times (Fig. S4 (b)) leads us to believe that in the recorded spectra we are dealing with a superposition of multiple spectral lines averaged over the exposure time.

References

1. Toropov, N., N. Leonov, and T. Vartanyan, *Influence of silver nanoparticles crystallinity on localized surface plasmons dephasing times.* physica status solidi (b), 2018. **255**(3): p. 1700174.
2. Wahl, M. and S. Orthaus-Müller, *Time tagged time-resolved fluorescence data collection in life sciences.* Technical Note. PicoQuant GmbH, Germany, 2014.
3. Campion, A. and P. Kambhampati, *Surface-enhanced Raman scattering.* Chemical society reviews, 1998. **27**(4): p. 241-250.
4. Kneipp, K. and H. Kneipp, *Single molecule Raman scattering.* applied spectroscopy, 2006. **60**(12): p. 322A-334A.
5. Jones, R.R., et al., *Raman techniques: fundamentals and frontiers.* Nanoscale research letters, 2019. **14**(1): p. 1-34.
6. Gunnarsson, L., et al., *Confined plasmons in nanofabricated single silver particle pairs: experimental observations of strong interparticle interactions.* The Journal of Physical Chemistry B, 2005. **109**(3): p. 1079-1087.
7. Savvin, A., et al., *NV–diamond laser.* Nature communications, 2021. **12**(1): p. 1-8.
8. Plakhotnik, T. and H. Aman, *NV-centers in nanodiamonds: How good they are.* Diamond and Related Materials, 2018. **82**: p. 87-95.
9. Vins, V. and E. Pestryakov, *Color centers in diamond crystals: Their potential use in tunable and femtosecond lasers.* Diamond and related materials, 2006. **15**(4-8): p. 569-571.